Chaotic Oscillation of a Piecewise-Constant System Realized by Switched-Capacitor Circuits

Tadashi TSUBONE and Noriyoshi KAMBAYASHI

Department of Electrical Engineering, Nagaoka University of Technology
1603-1 Kamitomioka-cho, Nagaoka, Niigata, 940-2188, Japan
Phone:+81-258-47-9558, Fax:+81-258-47-9500
Email: tsubone@vos.nagaokaut.ac.jp

1. Introduction

In this paper, we study a chaotic oscillator implemented by mean of switched-capacitor (abbr. SC) circuits. SC technique is useful and important for circuits realization on a chip as well known.

Many physical implementations of the chaos generator have been proposed, including IC chip implementations [1][2]. Such circuit can be exploited to consider basic problem of complex dynamic systems and engineering application, for example, chaos based communication systems [3].

On the other hand, since switches are nonlinear elements, nonlinear phenomena such as chaos and bifurcation are often observed in circuits with switches, for example, dc-to-dc converter [4][5]. The dynamics of switching circuits can be described by hybrid dynamics which contains both of continuous states and discrete states. Such hybrid systems is widely studied and the analysis of stability of the hybrid systems is important from engineering view point [6]. However, since general discussion of the hybrid systems is not easy, it is also important to consider a simple hybrid system which theoretical analysis is possible.

From these point of view, we consider a simple chaotic oscillator and its SC circuit implementation. And we analyze the stability of the oscillation. We aim to make a contribution toward synthesis and analysis for hybrid systems.

This paper is organized as the followings. Section 2 introduces a simple autonomous chaos generator; hysteresis piecewise-constant chaos generator. Piecewise-constant systems are extremely simple nonlinear systems and we have presented some theoretical results for analysis of bifurcations, chaos generations, and so on, in Ref. [7],[8] (and therein). We derive the condition of chaos generation of this circuit by using 1-D return map. Section 3 gives a SC implementation of the circuit introduced in sec. 2. This system is to be a higher order non autonomous circuit because a clock signal are applied to control switches. The system dynamics is described by 2-D difference equation which is represented by explicit form. We show the condition for attractor existence by using the similar way to 1-D return map procedure. Section 4 show a laboratory measurements of the SC circuit given in sec. 3. The experimental circuit is realized on Field Programmable Analog Array (abbr. FPAA) AN10E40 provided by Anadim Inc. Anadim chip AN10E40 is subdivided into 20 analog cells. Each analog cell consists of programmable capacitor banks, operational amplifiers, digitally controlled analog switches and so on. The analog cell is used as a basic SC component, for example, a integrator. Section 5 concludes the results and enumerates future problems.

2. Hysteresis piecewise-constant chaos generator

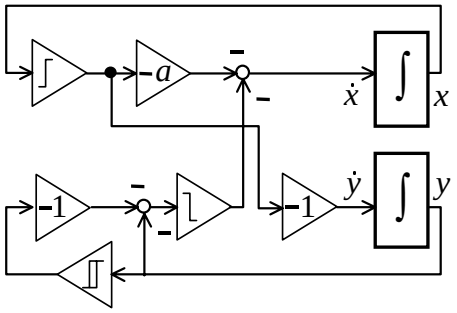

Figure 1: The system diagram.

The block diagram of the chaos generator is shown in Fig. 1 and the dynamics is described by the following differential equation:

$$\begin{cases} \dot{x} = a \cdot \mathrm{sgn}(x) + \mathrm{sgn}(y - h(y)), \\ \dot{y} = -\mathrm{sgn}(x), \end{cases} \qquad \mathrm{sgn}(x) \equiv \begin{cases} 1 & \text{for } x \geq 0, \\ -1 & \text{for } x < 0, \end{cases} \qquad h(x) \equiv \begin{cases} 1 & \text{for } x \geq -1, \\ -1 & \text{for } x < \quad 1, \end{cases} \tag{1}$$

where $h(x)$ is a normalized hysteresis: h is switches from 1 to -1 if x reaches 1 and vice versa. This system has only

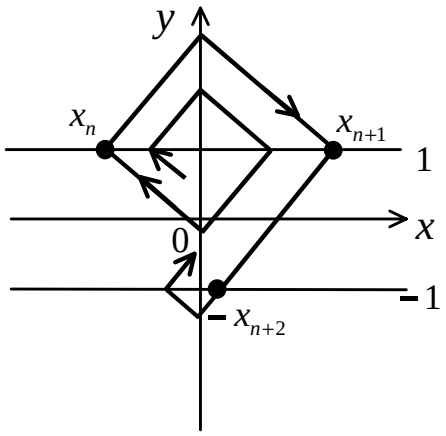

Figure 2: Trajectories on the phase space.

one parameter a and we assume $a > 0$ because, in this parameter range, the oscillation is guaranteed. Figure 2 shows the example of the system behavior. If h is 1, the trajectory moves divergently around $(0, 1)$. If the trajectory reaches $\{(x, y)|y = -1\}$, h is switches from 1 to -1 and the trajectory moves around $(0, -1)$. The system repeats this behavior.

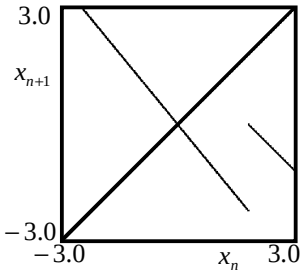

Figure 3: Return map ($a = 0.1$).

In order to analyze this system, we define 1-D return map. Let L_+ be $\{(x, y)|y = 1\}$, let L_- be $\{(x, y)|y = -1\}$ and let Th_1 be a x coordinates of a point on L_+ such that the trajectory starting from $(Th_1, 1)$ reaches straight to $(0, -1)$. Here we consider a trajectory starting from a point $(x_n, 1)$ on L_+. If $x_n \leq Th_1$, the trajectory returns to L_+ as shown in Fig. 2. If $x_n > Th_1$, the trajectory reaches straight to $(x_{n+1}, -1)$ on L_-. Here, noting that $(x_{n+1}, -1)$ on L_- is symmetric to $(-x_{n+1}, 1)$ on L_+, we can define 1-D return map from L_+ to L_+ that transforms x_n to x_{n+1}. Then the return map is formulated by

$$x_{n+1}{=}f(x_n){=}\begin{cases} -\dfrac{1+a}{1-a}x_n & \text{for } x_n \leq Th_1 \\ -(x_n - 2(1-a)) & \text{for } x_n > Th_1, \end{cases} \quad (2)$$

where $Th_1 = 2(1 - a)$. By using the return map, it is guaranteed that an attractor is exist if $f^3(Th_1) > f(Th_1)$, where f^n denotes the n-folds composition of f. Hence the condition for attractor existence is given by

$$0 < a < \sqrt{5} - 2. \quad (3)$$

In the condition (3), the attractor is chaos because $Df^2(x_n) > 1$ is satisfied for any x_n, where Df denotes the derivative of f.

3. Realization by switched-capacitor circuits

In this section, we consider the SC implementation of the system in sec. 2. The component blocks of the system diagram of Fig. 1 are realized by SC circuit with op-amp as shown in Fig. 4 $\sim$ Fig. 8. The switches of these circuits

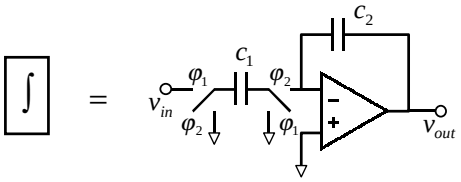

Figure 4: A noninverting integrator.

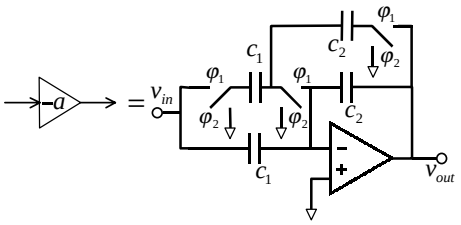

Figure 5: An inverting amplifier.

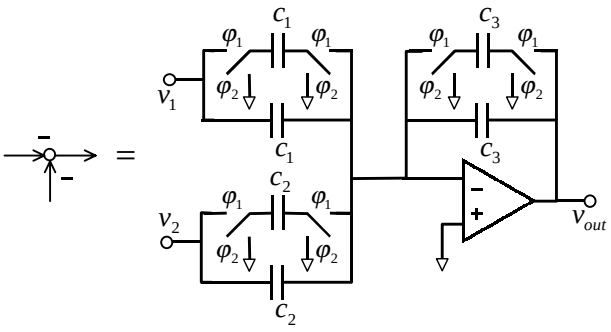

Figure 6: An inverting summer.

are controlled by non-overlapping clocks φ_1 and φ_2 with the period T as shown in Fig. 9. Using the appropriate transformations for the variables and the parameters, the circuit

dynamics is described by the following difference equation:

$$\begin{cases} x_{k+1} = x_k + \Delta T\{a \cdot \mathrm{sgn}(x_k) + \mathrm{sgn}(y_k - h(y_k))\} \\ y_{k+1} = y_k + \Delta T\{-\mathrm{sgn}(x_k)\}, \end{cases} \quad (4)$$

where ΔT is a parameter in proportion to T and a is mainly controlled the ratio of capacitance $\frac{c_1}{c_2}$ of the inverting amplifier. Figure 10 shows the behavior of the state variables of

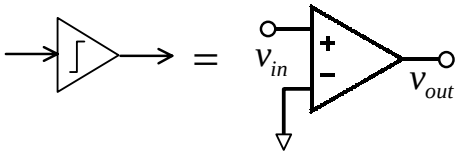

Figure 7: A comparator.

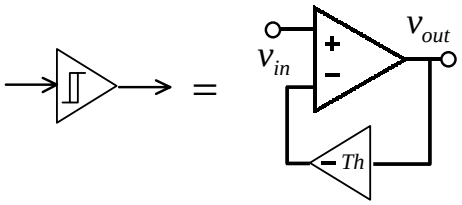

Figure 8: A hysteresis comparator.

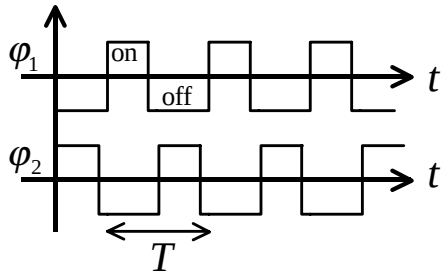

Figure 9: The clock signal controlling switches.

(4). If h is 1, the trajectory moves around $(0, 1)$ with expanding. If the trajectory crosses over $\{(x, y)|y = -1\}$, h is switches from 1 to -1 and the trajectory moves around $(0, -1)$. The system repeats this behavior.

In order to analyze the system, we derive the return map in similar way to sec. 2. Let L_+ be $\{(x, y)|y = 1\}$, let L_- be $\{(x, y)|y = -1\}$, and let $(\hat{x}_n, \hat{y}_n)$ be a point immediately after the trajectory crosses over L_+ or L_-, as shown in Fig. 10. The trajectory starting from $(\hat{x}_n, \hat{y}_n)$ must cross over L_+ or L_- again. Then we can define the map $\boldsymbol{F}$ that transforms a point $(\hat{x}_n, \hat{y}_n)$ to a point $(\hat{x}_{n+1}, \hat{y}_{n+1})$. Also letting $(\hat{x}'_n, \hat{y}'_n)$ be a point immediately after the trajectory crosses over L_-, the trajectory starting from $(\hat{x}'_n, \hat{y}'_n)$ is symmetric to the trajectory starting from $(-\hat{x}'_n, -\hat{y}'_n)$. Using the symmetric property, the map $\boldsymbol{F}$ is formulated by

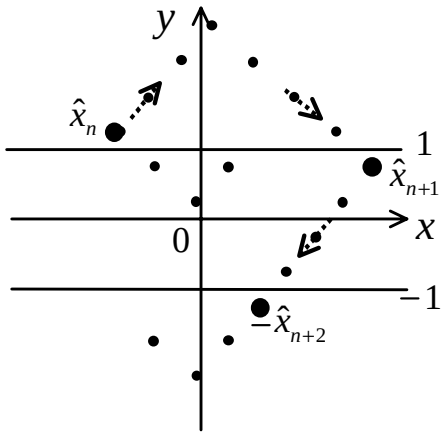

Figure 10: The trajectories on phase space.

$$\begin{cases} \hat{x}_{n+1} = \hat{x}_n + \left(2\left[\dfrac{-\hat{x}_n}{(1-a)\Delta T}\right] + 3 + a\right)\Delta T \\ \hat{y}_{n+1} = \hat{y}_n - \Delta T \end{cases}$$
for $(\hat{y}_n \geq 1)$ and $(\hat{x}_n < (1-a)\Delta T)$
$$\begin{cases} \hat{x}_{n+1} = \hat{x}_n - \left(2\left[\dfrac{\hat{x}_n}{(1-a)\Delta T}\right] + 3 + a\right)\Delta T \\ \hat{y}_{n+1} = \hat{y}_n + \Delta T \end{cases}$$
for $(Th_y \leq \hat{y}_n < 1)$ and $(\hat{x}_n < Th_x)$
or $(\hat{y}_n < Th_y)$ and $(\hat{x}_n < Th_x - (1-a)\Delta T)$
$$\begin{cases} \hat{x}_{n+1} = -\hat{x}_n + \left(2\left[\dfrac{2}{\Delta T}\right] + 1\right)(1-a)\Delta T \\ \hat{y}_{n+1} = -\hat{y}_n + \left(2\left[\dfrac{2}{\Delta T}\right] + 1\right)\Delta T \end{cases} \quad (5)$$
for $(Th_y \leq \hat{y}_n < 1)$ and $(\hat{x}_n \geq Th_x)$
$$\begin{cases} \hat{x}_{n+1} = -\hat{x}_n + \left(2\left[\dfrac{2}{\Delta T}\right]\right)(1-a)\Delta T \\ \hat{y}_{n+1} = -\hat{y}_n + \left(2\left[\dfrac{2}{\Delta T}\right]\right)\Delta T \end{cases}$$
for $(\hat{y}_n < Th_y)$ and $(\hat{x}_n \geq Th_x - (1-a)\Delta T)$

where $[\cdot]$ denotes a Gauss notation, $Th_x = [\frac{2}{\Delta T}](1-a)\Delta T$ and $Th_y = [\frac{2}{\Delta T}] - 1$. Figure 11 shows the relationship between $\hat{x}_n$ and $\hat{x}_{n+1}$. Note that $y_n \in [1 - \Delta T, 1 + \Delta T]$. Namely, in the case of $\Delta T \to 0$, the map $\boldsymbol{F}$ converges to the 1-D return map of (2).

Here using the relationship shown in Fig. 11, we derive the sufficient condition for attractor existence. If $\hat{x}_n < 0$, $\hat{x}_{n+1}$ is less than $g_1(\hat{x}_n) = -\frac{1+a}{1-a}\hat{x}_n + (3+a)\Delta T$. Also, if $0 < \hat{x}_n \leq Th_x$, $\hat{x}_{n+1}$ is grater than $g_2(\hat{x}_n) = -\frac{1+a}{1-a}\hat{x}_n - (3+a)\Delta T$. Furthermore, if $\hat{x}_n > Th_x$, the minimum $\hat{x}_{n+1}$ is given by $g_3(\hat{x}_n) = -\hat{x}_n + \left(2\left[\frac{2}{\Delta T}\right]\right)(1-a)\Delta T$. Hence, the the sufficient condition for attractor existence is given by

$$g_3(g_1(g_2(Th_x))) > g_2(Th_x). \quad (6)$$

In the case of $\Delta T \to 0$, the condition (6) is corresponded to the condition (2).

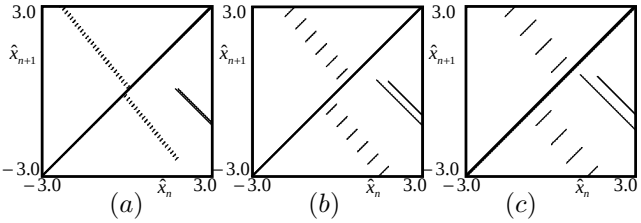

Figure 11: The relationship between $\hat{x}_n$ and $\hat{x}_{n+1}$ ($a = 0.1$, $(a)\Delta T = 0.1$, $(b)\Delta T = 0.4$, $(c)\Delta T = 0.6$).

4. FPAA realization

The system in sec. 3 is realized on FPAA (AN10E40) provided by Anadim Inc. Anadim chip AN10E40 is subdivided into 20 analog cells. The each circuit components in Fig. 4 $\sim$ Fig. 8 are implemented by using one or two the analog cells. In Fig. 12, the laboratory measurements are shown. In the theoretical sense, the attractors are not chaos because the absolute of the all eigen values of $\boldsymbol{DF}$ are 1. However the unstable oscillation is observed because of some perturbations.

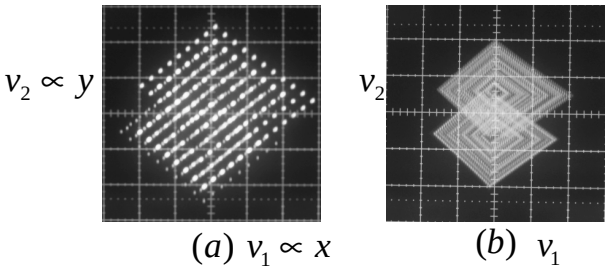

Figure 12: Typical attractors. ($a \simeq 0.05$, $(a)\Delta T \simeq 0.5, (\frac{1}{T} \simeq 20[\text{kHz}])$, $(b)\Delta T \simeq 0.05, (\frac{1}{T} \simeq 200[\text{kHz}])$)

5. conclusions

We considered a hysteresis piecewise-constant chaotic oscillator and its SC circuit implementation. And we analyzed the stability of the oscillation. First, we considered the continuous-time system and showed the condition for attractor existence and chaos generation by using 1-D return map. Second, we discussed the discrete-time system and also gave the condition for attractor existence by using the similar way to 1-D map procedure. Also, the discrete-time system was realized on FPAA and the oscillation are demonstrated. Finally, we enumerate future problems: 1) rigorous analysis of SC chaotic circuits, 2) systematic analysis of piecewise-constant systems.

References

[1] J. M. Cruz and L. O. Chua, "An IC Chip of Chua's Circuit," IEEE Trans., **CAS-II,** vol. 40, no. 10, pp. 614-625 (1998).

[2] M. Delgado-Restituto, M. Liñán and A. Rodoríguez-Vázquez, "CMOS 2.4μm Chaotic Oscillator: experimental verification of chaotic encryption of audio," *Electron Lett.*, vol. 32, no. 9, pp. 795-796 (1996)

[3] M. P. Kennedy, "Communicating with Chaos: State of the Art and Engineering Challenges," in *Proc. of IEEE/NDES'96*, Sevila, pp. 1-8, (1998)

[4] J. H. B. Deane and D. C. Hamill, "Modeling of chaotic DC-DC converters by iterated nonlinear mappings," *IEEE Trans.*, 7, pp. 25-36 (1992).

[5] G. Yuan, S. Banerjee, E. Ott and J. A. Yorke, "Border - Collision Bifurcations in Buck Converter," *IEEE Trans.*, **CAS-I**, vol. 45, no. 7, pp. 707-716 (1998).

[6] Special issue on Hybrid Control System, *IEEE Trans.*, **Auto. CTL**, vol. 43, no. 4, (1998).

[7] T. Tsubone and T. Saito, IEICE Trans., Fundamentals, vol. E82-A, no.8, pp.1619-1626 (1999).

[8] T. Tsubone, K. Hoshino and T. Saito, IEEE, proc. of ISCAS2001, pp.815-818, 2001.